

The Corrosion Inhibition of SS 41 Steel by Shoyu Oil

Isao SEKINE* and Masahiro ASAZUMA

Faculty of Science and Technology, Science University of Tokyo, Yamazaki, Noda, Chiba 278

(Received May 6, 1982)

The addition of shoyu (soy sauce) oil to an NaCl solution for use as a corrosion inhibitor of SS 41 steel was investigated by measuring the corrosion weight loss, the polarization curve, the polarization resistance, and the impedance of the metal-solution interface. The value of the weight loss and the double-layer capacitance, C_{dl} , decreased as the shoyu oil was added to NaCl solutions of various concentrations. The value of the corrosion current density, I_{corr} , as calculated from the weight loss, the polarization curve, and the impedance measurement, decreased with an increase in the concentration of shoyu oil. An efficient inhibition of the corrosion of SS 41 steel was observed above an additive concentration of about 0.3%. Thus, the shoyu oil was found to be useful as a corrosion inhibitor of an economical and anti-pollution type. From the results of the IR analysis, the inhibition of the shoyu oil was considered to be caused by the adsorption of fatty acids, especially unsaturated fatty acids involved in the shoyu oil.

It has been reported by Markina and Misler that the sodium soaps of synthetic fatty acids of C_5-C_6 , $C_{10}-C_{16}$, and $C_{17}-C_{20}$ are effective as corrosion inhibitors of 12Khl MF steel, which is a material used for boilers.¹⁾ The corrosion-inhibition effect by the adsorption of amine salts of oleic acid on iron in 0.5 M H_2SO_4 (1 M = 1 mol dm⁻³) has been discussed by Szauer and Brandt.^{2,3)} According to some articles,⁴⁻⁶⁾ fatty acid with $C_{16}-C_{18}$ atoms has been considered as exerting the most effective inhibition. Such a corrosion-protection effect is caused by the adsorption of the anion of fatty acid or the cation of amine. The adsorption in this case is known to obey the Frumkin or Temkin isotherm. Further, the adsorption of fatty acid shows a tendency to increase with an increase in the length of the aliphatic chain, while the inhibition effect shows a tendency to decrease with an increase in the number of the double bond of fatty acid.^{2,3)}

In the present work, we examined the use of shoyu oil added to an NaCl solution as a corrosion inhibitor of metal, for example, SS 41 steel. Since this oil is a by-product of shoyu production and a mixture of five kinds of natural fatty acids with $C_{16}-C_{18}$ atoms, it was expected to be useful and economical as a corrosion inhibitor of an anti-pollution type. Thus, the inhibition effect of the shoyu oil was investigated by measuring the weight loss, the polarization curve, the interfacial impedance, and the polarization resistance in a neutral NaCl solution. From the results obtained, it was found that the shoyu oil inhibits the corrosion of SS 41 steel sufficiently and can be used satisfactorily as an inhibitor of corrosion by cooling water and industrial water. The corrosion inhibition of shoyu oil was considered, from the results of the IR reflection spectrum, to be caused by the adsorption of the anion of fatty acid.

Experimental

Materials. The shoyu oil used as a corrosion inhibitor was from intact soybeans and defatted soybeans. Since these shoyu oils are insoluble in water, soluble sodium salts of them were prepared according to the procedure shown in Fig. 1. The sodium salt of shoyu oil from intact soybeans is abbreviated as SSOI, and the sodium salt of shoyu oil from defatted soybeans, as SSOD. The compositions of these SSOI and SSOD are shown in Table 1. This table shows that the shoyu oils consist of about 80% unsaturated

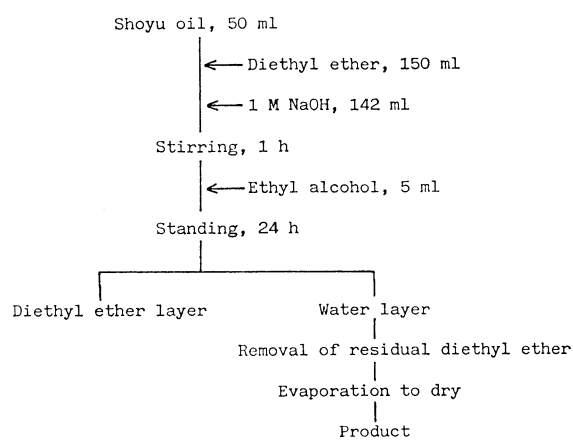


Fig. 1. Preparation of sodium salt of shoyu oil.

TABLE 1. COMPOSITIONS OF SSOI AND SSOD

Sodium salt of fatty acid	SSOI(%)	SSOD(%)
$C_{15}H_{31}COONa$	10.7	16.7
$C_{17}H_{35}COONa$	9.2	6.1
$C_{17}H_{33}COONa$	17.6	27.8
$C_{17}H_{31}COONa$	55.2	45.7
$C_{17}H_{29}COONa$	7.4	3.7

fatty acids and of about 20% saturated fatty acids. The concentrations of the NaCl solutions used as blank solutions were 0.003, 0.03, 0.3, and 3%. The concentrations of these inhibitors were 0.1, 0.3, 0.5, and 1.0% respectively. Before each run, all the solutions were sufficiently aerated and adjusted to pH 7. The specimen used was SS 41 steel.

Weight-loss Measurement. The specimen sheet of 25 × 60 × 0.5 mm was immersed in the test solution for five weeks at room temperature. Before use, the specimen was abraded with emery papers from No. 240 to No. 1200, and successively washed with distilled water, methanol, and acetone. In the corrosion weight-loss test at high temperature, the weight loss of the specimen was measured after the specimen had been immersed in a test solution maintained at 95 °C for 3 d. The boiling point of the test solution was 95 °C.

Polarization Measurement. A specimen wire 1 mm in diameter was covered with a mixture of paraffin wax and pine resin, and only the cross-section of the specimen was used. The counter electrode was a platinum wire, while the potential was measured with reference to a saturated calomel electrode (SCE). The polarization potentials were scanned from the cathodic region to the anodic region.

Impedance Measurement. The specimen used was the same as that used in the polarization measurement. The corrosion potential, E_{corr} , of the test electrode was stabilized 1–2 h after immersion. Thus, the measurements of the impedance were started when the E_{corr} value was stabilized. In the frequency range of 2 kHz–1 Hz, a lock-in amplifier (NF Circuit Design Block; model LI-574) was used, while in the frequency range of 1 Hz–0.006 Hz, Lissajou's method was used.

Polarization-resistance Measurement. A specimen rod 4 mm in diameter was covered with pine resin except for the bottom 30 mm. The measurement was made by using a corrosion-rate meter (Hokuto Denko; model HK-103). The frequency and time of measurement were 0.1 Hz and 110 h respectively.

IR Analysis. Before the IR analysis, the specimen sheet taken out from the test solution to measure its corrosion weight loss was vacuum-dried for about 30 min. The angle of incidence was 12°, and the number of reflections was one.

Results and Discussion

The weight loss against the concentration of SSOI is shown in Fig. 2. As may be seen in this figure, the value of the weight loss was lowered with an increase in the concentration of SSOI and held constant in concentrations more than 0.3%. Such a tendency was also seen for SSOD. In any concentration of NaCl solution used, the surface of test pieces in the blank solution became dark brown, and then a reddish-brown precipitate in the solution was observed. However, the test pieces immersed in solutions with concentration over 0.3% of SSOI and 0.5% of SSOD kept the same silvery metallic luster as before immersion. Such a surface state may be seen in Photo 1.

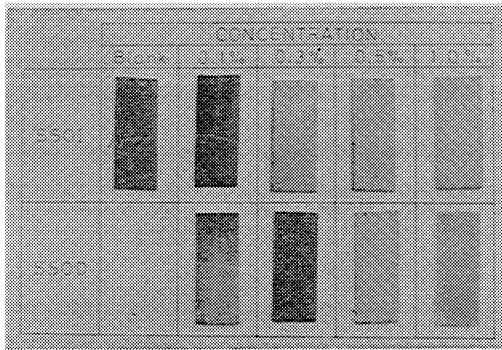


Photo 1. Surface state of specimen after corrosion weight loss for various concentrations of SSOI and SSOD in 3% NaCl solution at room temperature.

Figure 3 shows a comparison between the shoyu oil and other inhibitors. Sodium benzoate (SB) and sodium *p*-*t*-butylbenzoate (SBB) have been used as corrosion inhibitors for a long time. As can be seen from this figure, the outstanding inhibitive effectiveness at a concentration over 0.3% of SSOI added to a 0.003% NaCl solution was comparable to that of SB and SBB.

Table 2 shows the results of the weight-loss test at 95 °C from the viewpoint of practical utilization. In general, when an inhibitor is used, the adjustment

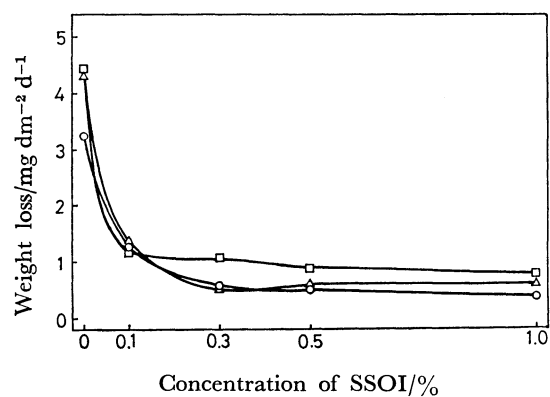


Fig. 2. Corrosion weight loss *vs.* concentration of SSOI curves in various concentrations of NaCl solution.
—○—: 0.03%, —△—: 0.3%, —□—: 3%.

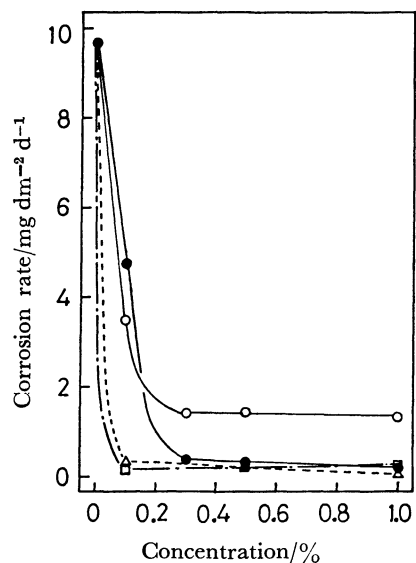


Fig. 3. Corrosion weight loss *vs.* concentration of various inhibitors in 0.003% NaCl solution.
—○—: SSOD, —●—: SSOI, —△—: SB, —□—: SBB.

TABLE 2. CORROSION WEIGHT LOSS AT 95 °C

	Solution	pH	Weight loss mg dm⁻² d⁻¹
Blank	0.003% NaCl	7.00	26.5
Natural	0.1% SSOI	10.28	3.67
	0.5% SSOI	10.72	0.87
	1% SSOI	10.90	0.22
	1% SSOD	11.10	2.32
Synthetic	1% SSOI	9.66	8.72
	1% SSOD	9.90	6.65
Comparative	1% C ₁₅ H ₃₁ COONa	10.03	0.74
	1% C ₁₇ H ₃₅ COONa	10.15	3.37
	1% C ₁₇ H ₃₃ COONa	10.30	8.94
	1% C ₁₇ H ₃₁ COONa	10.15	9.67
	1% C ₁₇ H ₂₉ COONa	10.55	1.68
	1% C ₆ H ₅ COONa	11.00	1.01
	1% C ₅ H ₁₁ COONa-C ₄ H ₉ COONa	6.62	13.4

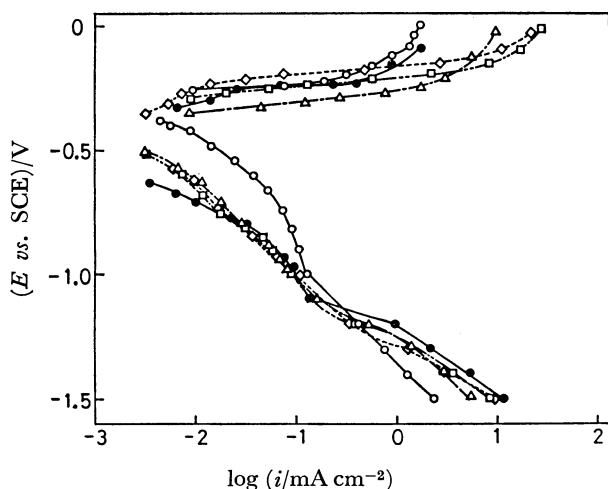


Fig. 4. Polarization curves for SSOD in 0.003% NaCl solution.

—○—: Blank, ---△---: 0.1% SSOD, ---□---: 0.3%, ---◇---: 0.5%, —●—: 1.0%.

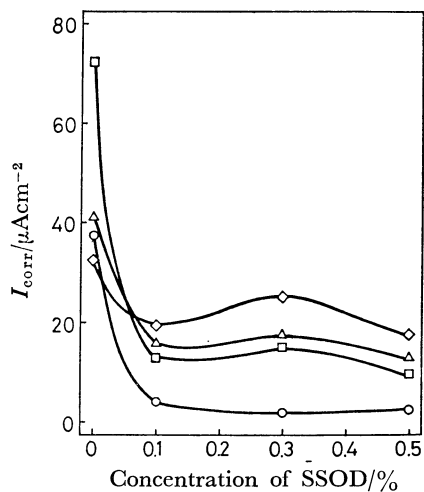


Fig. 5. I_{corr} vs. concentrations of SSOD curves in various concentrations of NaCl solution.

—○—: 0.003%, —△—: 0.03%, —□—: 0.3%, —◇—: 3%.

of the pH is very troublesome. Consequently, all runs at 95 °C were carried out without adjusting the pH. This table further compares the natural shoyu oil as a by-product, the synthetic shoyu oil prepared by mixing all the components of Table 1, sodium salt of five fatty acids containing the components of shoyu oil, and the fatty acids with C_5 – C_6 atoms reported by Markina *et al.*¹⁾ As can be seen in this table, among all the inhibitors under investigation, natural SSOI is the most efficient. The natural SSOD is less effective than SSOI, as can be seen from Photo 1. However, it seems that both SSOI and SSOD are efficient corrosion inhibitors in view of the utilization of by-products.

The polarization curves for SS 41 steel in a 0.003% NaCl solution containing SSOD are shown in Fig. 4. The current density of the cathodic process decreases with an increase in the concentration of SSOD, and the E_{corr} shifts to the direction of the cathodic

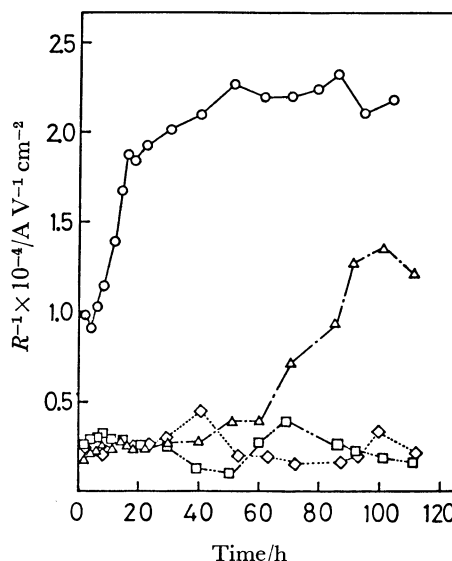


Fig. 6. $1/R$ vs. time curves in 0.003% NaCl solution.

—○—: Blank, ---△---: 0.1% SSOI, ---□---: 0.3%, ---◇---: 1.0%.

region. In general, when oxygen is dissolved in a neutral solution, the corrosion rate is determined by the limiting current density due to oxygen reduction. The decrease in the cathodic current density with an increase in the concentration of inhibitors indicates a lowering of the corrosion rate.

The relationship between the I_{corr} value and the concentration of SSOD is shown in Fig. 5. At each concentration of NaCl solutions, the I_{corr} value can be seen to decrease with an increase in the concentration of SSOD. Consequently, the SSOD is regarded as a good corrosion inhibitor. However, the I_{corr} value shows something of a tendency to increase at the concentration of 0.3% of SSOD. Since the determination of I_{corr} from the polarization curves is arbitrary, such a tendency may be attributed to the method of drawing the line.

Figure 6 shows the time dependence of $1/R$, which is the quantity corresponding to the corrosion rate ($I_{\text{corr}} = K/R$). The value of $1/R$ decreases with an increase in the concentration of SSOI. Especially at a concentration over 0.3% of SSOI, it is seen to be lowered for a long time. A similar result was also obtained for SSOD. From these results, it is considered that both SSOI and SSOD are fairly sufficient inhibitors.

Some typical results of impedance measurements at E_{corr} are shown in Fig. 7. In a high-frequency region, the loci of the circular arcs are seen to be a part of a semicircle whose center is shifted under the real axis. On the other hand, straight lines with a slope of about 45° are obtained in the low-frequency region. The charge-transfer resistance, R_{ct} , obtained by the extrapolation of a part of the semicircle to the real axis was about 850 Ω at the blank solution and about 1 kΩ at the solution with 0.3% SSOD added. The straight lines in the low-frequency region seem to be based on the diffusion of oxygen, because all the solutions used are aerated before each run. Consequent-

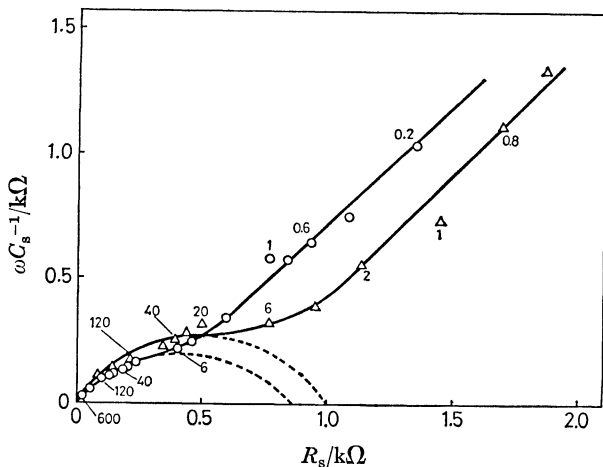


Fig. 7. Complex impedance plane plot at E_{corr} in 3% NaCl solution.
 —○—: Blank, —△—: 0.3% SSOD.

TABLE 3. COMPARISON OF THE RESULTS OBTAINED IN A 3% NaCl SOLUTION

SSOD %	Impedance measurement			Weight loss I_{corr} $\mu\text{A cm}^{-2}$	$i-E$ curve I_{corr} $\mu\text{A cm}^{-2}$
	R_{ct} Ω	C_{dl} $\mu\text{F cm}^{-2}$	I_{corr} $\mu\text{A cm}^{-2}$		
0	850	3980	1290	106.0	35
0.1	950	2130	1160	29.1	19
0.3	1000	1010	1100	18.9	26
0.5	1080	470	1020	17.4	17

ly, the diffusion process of oxygen is the rate-determining step. The value of C_{dl} calculated from Fig. 7 was about $4000 \mu\text{F/cm}^2$ at the blank solution and about $1000 \mu\text{F/cm}^2$ at 0.3% SSOD.

Table 3 shows the values of R_{ct} , C_{dl} , and I_{corr} against each concentration of SSOD. It can be seen that the R_{ct} value increases with an increase in the concentration of SSOD, while the C_{dl} value decreases. When the R_{ct} values, that is, the reaction resistance of corrosion, becomes greater, the SSOD seems to be the better inhibitor. On the other hand, the decrease in C_{dl} can be seen to be based on a reduction of the surface area of the specimen by a corrosion inhibitor. This can be explained by means of a Helmholtz parallel-plate condenser model:⁷⁾

$$C_{\text{dl}} = C_{\text{H}} = \epsilon(S/d),$$

where C_{H} is the Helmholtz capacity; S , the area of the condenser plates opposite to each other; d , the distance between the condenser plates, and ϵ , the dielectric constant. These results seem to be evident, for the SSOD leads to an efficient inhibition with an increase in the concentration of SSOD. Further, the values of I_{corr} , as calculated from the polarization curve, correspond very well with those calculated from the weight loss. However, these I_{corr} values differ very much from those calculated from the impedance measurement. This discrepancy can be ascribed to the fact that the determination of R_{ct} is very difficult, because the center of the semicircle obtained is shifted under the real axis. Therefore, the I_{corr} value with

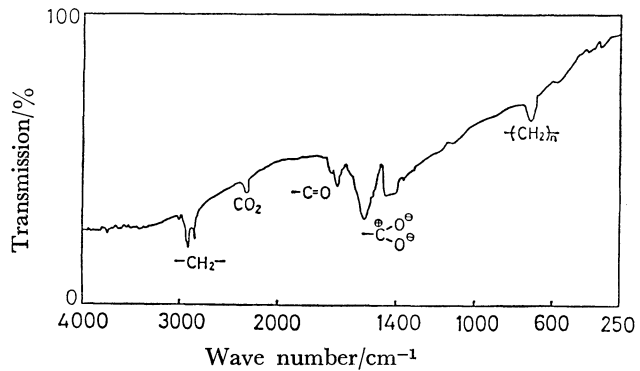


Fig. 8. Result of reflection type IR spectrum in 0.3% NaCl solution with 0.3% SSOD.

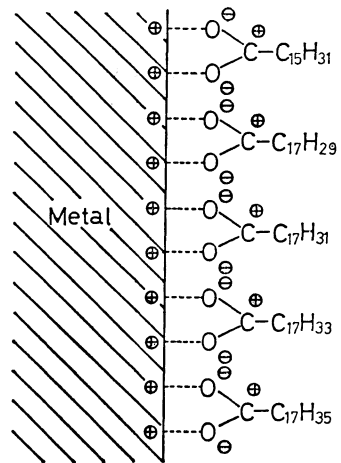


Fig. 9. Adsorption model of SSOI and SSOD.

respect to R_{ct} may be considered to admit of further argument.

The inhibition mechanism of SSOI was examined by means of infrared analysis. An example of the spectrum of the IR reflection type is shown in Fig. 8. It shows the spectrum of a specimen immersed for 3 d in a 0.3% NaCl solution containing 0.3% SSOI. In the IR spectrum, the two peaks at 2850 and 2900 cm^{-1} represent the stretching vibration of -C-H of the methylene group; the peak at 1700 cm^{-1} , that of aliphatic carboxylic acid; the two peaks from 1400 to 1600 cm^{-1} , that of the carboxylate ion, and the peak at 700 cm^{-1} , the rocking vibration of the polymethylene chain. Consequently, the adsorption model of SSOI and SSOD is roughly represented in Fig. 9. According to Szauer and Brandt,²⁾ when the unsaturated fatty acids of C_{18} were used as corrosion inhibitors, the effect of corrosion inhibition is related to the number of the double bond of fatty acid, and the inhibition effect decreases with an increase in the number of the double bond in the order of oleic acid > linoleic acid > linolenic acid. This is considered to be caused by the influence of π electrons in the double bond. In the present study, the adsorption seems to occur in two steps.⁸⁾ At first, the hydrophilic carboxylate ions adsorb on the metal surface. Subsequently, the hydrophobic alkyl groups are vertically oriented to the metal surface toward the bulk solution. How-

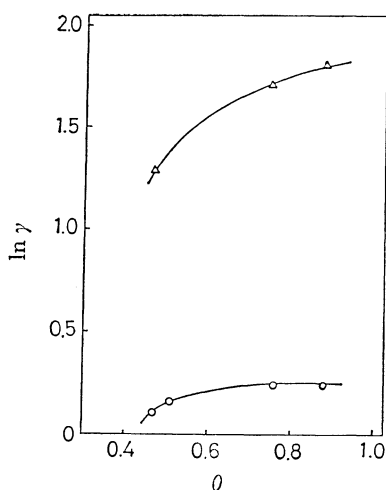


Fig. 10. Dependence of logarithm of inhibition coefficient on surface coverage for iron dissolution.
—○—: Impedance measurement, —△—: weight loss.

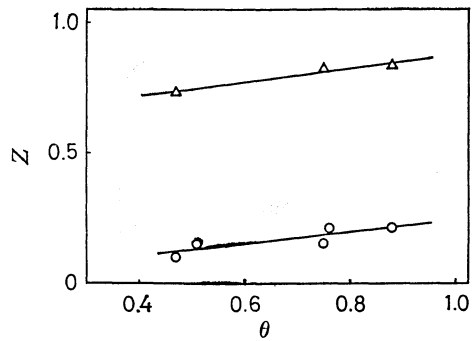


Fig. 11. Inhibition efficiency of iron dissolution vs. surface coverage.
—○—: Impedance measurement, —△—: weight loss.

ever, when the double bond is involved in fatty acid, the alkyl groups are bent to the metal surface by the influence of π electrons in the double bond, and then corrosive chemical species (Cl^- , O_2 , H_2O , etc.) come near to the metal surface. Therefore, it is considered that the inhibition effect decreases with an increase in the number of double bonds. As may be seen in Table 2, linolenic acid exerts the most efficient inhibition compared with the other unsaturated fatty acids. These results differ from those described by Szauer and Brandt.²⁾ Hence, in order to clarify such a discrepancy, further work would be required from the standpoint of the influence of the double bond.

According to Wolstenholme and Schulman,⁹⁾ fatty acid does not simply adsorb on the metal surface, as is represented in Fig. 9, but makes a complex with the iron ion which grows relatively thick. However, the adsorption model in Fig. 9 may be supposed to show not only unsaturated fatty acids, but also saturated ones such as stearic acid, because it is impossible to discriminate the carboxylate ions of both fatty acids by IR analysis. As can be seen from Table 1, since the shoyu oil consists of about 80% unsaturated fatty acids, the adsorption of SSOI and SSOD would be caused chiefly by unsaturated fatty acids. Hence, the adsorption model of shoyu oil shown roughly in

Fig. 9 may be considered to be reasonable.

It is generally known that the adsorption of fatty acids on iron obeys Frumkin-Temkin's isotherm. In the present work, the adsorption of shoyu oil is also assumed to obey Frumkin-Temkin's isotherm. Thus, we investigated whether the adsorption is chemisorption or physical adsorption. According to Reshetnikov,¹⁰⁾ when the inhibition takes place by means of physical adsorption, Eq. 1 is valid without chemisorption, and the inhibition by chemisorption satisfies Eq. 2:

$$\ln \gamma = m\theta \quad (1)$$

$$Z = 1 - \frac{1}{\gamma} = \theta, \quad (2)$$

where γ is the inhibition coefficient which is defined by the relation $\gamma = k/k_{inh}$; k and k_{inh} , the rates of iron dissolution in the absence and presence of the inhibitor respectively; Z , the inhibition efficiency; θ , the surface coverage calculated on the basis of the capacitance measurement, and m , the constant. In the present study γ and Z were calculated from I_{corr} , which has itself been obtained from the measurements of the impedance and the weight loss, and θ is the value of C_{dl} at E_{corr} obtained from the impedance measurement.

Figures 10 and 11 show the results plotted for SSOD according to Eqs. 1 and 2. In Fig. 10 the linearity of $\ln \gamma$ vs. θ can not be seen, but the plots of Z vs. θ in Fig. 11 give a straight line. Consequently, the adsorption in the case of SSOD is regarded as chemisorption.

In order to elucidate more clearly the adsorption state of these inhibitors, there seems to be no alternative but to wait for future work *in situ* by means of optical methods.

The authors are very grateful to Professor Zenjiro Sugizaki of our university for his useful suggestions and to the Kikkoman Co. for the gift of a shoyu oil sample. The authors also wish to thank Messrs. Toshiki Mitsuka, Hiroyuki Mizoguchi, and Hideaki Sako for carrying out a part of the experiments.

References

- 1) M. V. Markina and Zh. V. Misler, *Zashch. Met.*, **14**, 95 (1978).
- 2) T. Szauer and A. Brandt, *Electrochim. Acta*, **26**, 1209 (1981).
- 3) T. Szauer and A. Brandt, *Electrochim. Acta*, **26**, 1219 (1981).
- 4) H. F. Finley and N. Hackerman, *J. Electrochem. Soc.*, **107**, 259 (1960).
- 5) R. J. Meakins, *J. Appl. Chem.*, **13**, 399 (1963).
- 6) M. Smialowski, T. Ostrowska, and Z. Szklarska-Smialowska, *Roczn. Chem.*, **29**, 674 (1955).
- 7) I. Sekine and H. Ohkawa, *Bull. Chem. Soc. Jpn.*, **52**, 2853 (1979).
- 8) N. Hackerman and A. C. Makrides, *Ind. Eng. Chem.*, **46**, 523 (1954).
- 9) G. A. Wolstenholme and J. H. Schulman, *Trans. Faraday Soc.*, **46**, 475 (1950).
- 10) S. M. Reshetnikov, *Zashch. Met.*, **14**, 597 (1978).